JCTC Journal of Chemical Theory and Computation

Ligand Affinities Estimated by Quantum Chemical Calculations

Pär Söderhjelm,[†] Jacob Kongsted,[‡] and Ulf Ryde*,[†]

Department of Theoretical Chemistry, Lund University, Chemical Centre, P.O. Box 124, 221 00 Lund, Sweden, and Department of Physics and Chemistry, University of Southern Denmark, Campusvej 55, 5230 Odense M, Denmark

Received December 30, 2009

Abstract: We present quantum chemical estimates of ligand-binding affinities performed, for the first time, at a level of theory for which there is a hope that dispersion and polarization effects are properly accounted for (MP2/cc-pVTZ) and at the same time effects of solvation, entropy, and sampling are included. We have studied the binding of seven biotin analogues to the avidin tetramer. The calculations have been performed by the recently developed PMISP approach (polarizable multipole interactions with supermolecular pairs), which treats electrostatic interactions by multipoles up to quadrupoles, induction by anisotropic polarizabilities, and nonclassical interactions (dispersion, exchange repulsion, etc.) by explicit quantum chemical calculations, using a fragmentation approach, except for long-range interactions that are treated by standard molecular-mechanics Lennard-Jones terms. In order to include effects of sampling, 10 snapshots from a molecular dynamics simulation are studied for each biotin analogue. Solvation energies are estimated by the polarized continuum model (PCM), coupled to the multipole-polarizability model. Entropy effects are estimated from vibrational frequencies, calculated at the molecular mechanics level. We encounter several problems, not previously discussed, illustrating that we are first to apply such a method. For example, the PCM model is, in the present implementation, questionable for large molecules, owing to the use of a surface definition that gives numerous small cavities in a protein.

Introduction

A major goal within theoretical chemistry is to accurately predict the free energy for the binding of a ligand to a macromolecule. If such binding affinities could be accurately predicted, large parts of the drug development could be performed by computer simulations rather than by costly experiments, because essentially all drugs evoke their action by binding to a target macromolecule. Likewise, many interesting questions in biochemistry can be formulated as the differential binding affinities of a substrate, product, or transition state to a protein or enzyme.

Consequently, numerous theoretical methods have been developed to estimate ligand affinities.[1] The most accurate ones are based on free-energy perturbation (FEP) and related approaches.[2] Unfortunately, they are extremely time-consuming, and the results typically converge only when the difference in binding affinity of similar ligands is considered, i.e., for relative binding affinities. Therefore, many more approximate methods have been suggested. Some of them are still based on extensive sampling of the phase space, e.g., linear-response approximation (LRA), the semimacroscopic protein-dipole Langevin-dipole approach (PDLD/S-LRA), the linear interaction energy (LIE), and molecular mechanics Poisson−Boltzmann surface area (MM/PBSA) approaches.[3−7] Other methods use a single molecular conformation and estimate the binding affinities by methods based on either physics or statistics.[1]

Most of the physical methods are based on calculations with a molecular mechanics (MM) force field. These force fields enable fast energy evaluations that allow extensive sampling. Moreover, they have the advantage of being

* Corresponding author e-mail:Ulf.Ryde@teokem.lu.se.
[†] Lund University.
[‡] University of Southern Denmark.

10.1021/ct9006986
Published on Web 04/15/2010

tunable for specific systems and allowing contributions from the surrounding solvent to be included in an effective way through parametrization. Nevertheless, although the accuracy of ligand-affinity calculations is often limited by the extent of phase-space sampling, it can also be limited by the accuracy of the underlying force field. The deviation from experimental results seen even in well-converged free-energy calculations has often been attributed to imperfect force fields.[8] In fact, the results obtained with various MM force fields may differ strongly; for example, for biotin binding to avidin, there was a 91 kJ/mol difference in the interaction energy calculated with the Amber 1994 and 2002 force fields.[9] Likewise, FEP estimates of the binding affinities of five ligands to serine proteases differed by up to 36 kJ/mol between the MMFF and QMPFF force fields.[10] From a more conceptual point of view, it is also valuable to use an energy function that is less empirical, so that the results depend less on error cancellation.

Therefore, there has recently been great interest in developing ligand-binding methods that are based on quantum mechanics (QM), rather than on a MM force field.[11] Such methods are typically based on either semiempirical calculations[12,13] or on higher-level methods, using fractionation approaches, e.g., the fragment molecular orbital method (FMO)[14,15] or the molecular fractionation with conjugate caps (MFCC) and related methods.[16−22] However, it is well-known that calculations of dispersion effects generally require a very high level of theory.[23] Likewise, accurate predictions of polarization and dispersion effects require the use of a large and flexible one-electron basis set.[23,24] Only one of these previous studies[22] has been performed at a level (MP2/6-311(+)G(2d,p)) for which there is hope that dispersion and polarization effects are treated in a balanced and satisfactory way.

Recently, we have developed an approach that is intended to provide accurate interaction energies between a ligand and a macromolecule at a proper level of theory.[9] It is called PMISP (polarizable multipole interactions with supermolecular pairs). It treats electrostatic interactions by multipoles up to quadrupoles, induction by anisotropic polarizabilities, and nonclassical interactions (dispersion, exchange repulsion, etc.) by explicit quantum mechanical calculations, using a fragmentation approach similar to MFCC. It has given an accuracy of 2−5 kJ/mol for neutral and ∼10 kJ/mol for charged ligands compared to a full QM treatment.[9] This error could be reduced to 5 and 3 kJ/mol if the Hartree−Fock (HF) calculation for the full system is possible. For calculations with a whole protein, much computer time can be saved if long-range interactions are treated by a QM/MM approach (PMISP/MM).[25] If the boundary between the PMISP and MM systems is chosen far enough from the ligand, this approximation does not add any additional uncertainty. By this approach, we have illustrated the importance of using a proper level of theory. For example, the difference in interaction energy between two biotin analogues binding to avidin varied by 108 kJ/mol depending on the basis set employed (6-31G* or aug-cc-pVTZ at the MP2 level).[25]

However, in order to provide reliable ligand-binding energies, more terms than the pure interaction energy need to be considered. In particular, the effects of the surrounding solvent, entropy, and sampling need to be taken into account.[1,7] Only a few of the previous attempts to calculate ligand-binding energies with pure QM methods[12−22] have taken into account effects of solvation[12,13,15] (by a self-consistent reaction field Poisson−Boltzmann model and a surface area model) and entropy[12,13] (by counting the number of rotable bonds that are fixed during binding), and none of them consider sampling.

In this paper, we present what seems to be the first realistic QM estimation of ligand-binding affinities at a proper level of theory and at the same time taking into account the combined effects of solvation, entropy, and sampling. We employ the PMISP/MM method at the MP2/cc-pVTZ level within the framework of the MM/PBSA approach. We study the affinities of seven biotin analogues to the full avidin tetramer. This system is well characterized by X-ray crystallography,[26−29] and experimental binding free energies for a number of ligands (biotin analogues) are available.[30−32] Moreover, it has been investigated using several different theoretical methods.[33−39]

Methods

The PMISP/MM Method. The PMISP and PMISP/MM approaches have previously been thoroughly described.[9,25] Therefore, we here only provide a short summary of the methods. We consider the binding of a ligand (L) to a protein (P):

$$\mathrm{P} + \mathrm{L} \rightarrow \mathrm{PL} \tag{1}$$

In the PMISP method,[9] the interaction energy is estimated by

$$E_{\mathrm{PMISP}}(\mathrm{PL}) = E_{\mathrm{es}}(\mathrm{PL}) + E_{\mathrm{ind}}(\mathrm{PL}) + E_{\mathrm{nc}}(\mathrm{PL}) \tag{2}$$

where E_{es} and E_{ind} are the electrostatic and induction interaction energies, respectively. All energies in eqs 2−4 are interaction energies between L and P, not the absolute energies of the PL complex. The term E_{es} is calculated from a multicenter−multipole expansion up to quadrupoles, centered at all atoms and bond midpoints in the protein and the ligand. Likewise, E_{ind} is calculated from anisotropic dipole polarizabilities in the same centers in a self-consistent manner. Both these terms are obtained with the LoProp approach.[40] E_{nc} is the nonclassical term, containing mainly dispersion and exchange repulsion but also short-range corrections to the classical terms, e.g., charge penetration. It is estimated by

$$E_{\mathrm{nc}}(\mathrm{PL}) = \sum_{i=1}^{n} c_i (E_{\mathrm{QM}}(\mathrm{P}_i\mathrm{L}) - E_{\mathrm{es}}(\mathrm{P}_i\mathrm{L}) - E_{\mathrm{ind}}(\mathrm{P}_i\mathrm{L})) \tag{3}$$

where the protein has been divided into a number of fragments (P_i), using the molecular fractionation with conjugate caps (MFCC) method.[41] In this paper, each amino acid constitutes one fragment, and they are capped with CH_3CO- and $-NHCH_3$ groups. The caps from neighboring fragments are joined to form a $CH_3CONHCH_3$ conjugated cap (concap) for each peptide bond, and the energies of these

concaps are subtracted ($c_i = -1$ in eq 3) from the energies of the capped amino acid fragments ($c_i = 1$). This has been shown to be an excellent approximation, giving errors of only ~1 kJ/mol.[9] $E_{QM}(P_iL)$ is the counterpoise-corrected quantum mechanical (QM) interaction energy of the P_i-L pair. A similar formula is used to derive properties (multipoles and polarizabilities) for the whole protein from fragment-wise calculations.[9] E_{QM} was calculated at the MP2/cc-pVTZ level, which has been shown to provide dispersion energies similar to coupled-cluster methods with larger basis sets, owing to error cancellation.[25,42] The multipoles and polarizabilities were calculated at the B3LYP/6-31G* level, which has been shown to be a good approximation for the much more expensive MP2/cc-pVTZ properties, provided that the same properties are used in both eqs 2 and 3.[25]

For a large protein, only a few fragments P_i are in close contact with the ligand, so the direct use of eq 2 would be very inefficient. Therefore, we can save much time without compromising the accuracy by using a QM/MM approach, PMISP/MM:[25] For a model containing residues close to the ligand (M), the full PMISP approach is used, whereas for more distant residues, E_{nc} is approximated by the Lennard-Jones term from a classical force field, E_{LJ}:

$$E_{PMISP/MM}(PL) = E_{es}(PL) + E_{ind}(PL) + E_{nc}(ML) + E_{LJ}(PL) - E_{LJ}(ML) \quad (4)$$

Thus, we use the same accurate multipole-polarizability model for the whole protein. In this work, the E_{LJ} term is taken from the Amber 1994 force field (the same terms are also used in the newer Amber 2003 and the polarizable 2002 force fields).[43−45] Naturally, the accuracy of this approximation will improve as the size of the M region is increased.[25] In this work, we have used all atoms that are within 4 Å of the ligand in at least one snapshot and added enough atoms to obtain chemically reasonable groups, such as aromatic rings or amide groups. For groups that form exceptionally strong interactions with the ligand (distances shorter than 1.7 Å), the model was extended with an extra CH_2 group, to avoid the largest errors observed previously[25] (e.g., Ser-73 was modeled by ethanol, rather than methanol). Thus, M consisted of 165−271 atoms, depending on the ligand (but the same M region was used for all snapshots with the same ligand).

It was previously shown that the PMISP error is rather insensitive to the quantum-chemical method and basis set employed and thus that one can exploit error cancellation.[9] Therefore, we also performed PMISP and full supermolecular calculations for the M region of each snapshot at a lower level of theory, HF/6-31G*, and subtracted the resulting deviation from the E_{nc}(ML) term. The average correction was 6 kJ/mol, i.e., similar to the errors observed before for the same systems but with snapshots taken from a simulation with another force field.[9] By this procedure, the estimated error compared to full MP2/cc-pVTZ calculations is reduced to 3 kJ/mol for the M region,[9] whereas the protein environment adds an uncertainty of 5−8 kJ/mol.[25] All PMISP calculations were performed with the Molcas 7.2 software,[46] applying the Cholesky decomposition approximation to the two-electron integrals[47,48] in combination with the local-exchange algorithm.[49] We confirmed that the decomposition threshold used (10^{-4}) gave less than 1 kJ/mol error in the interaction energies.

PMISP/MM differs in several respects from standard QM/MM methods.[50] First, it uses a polarizable MM force field, which has been used in some previous studies[50,51] but is not routinely used. Second, a more advanced MM potential is used for the electrostatic interactions, including multipoles up to quadrupoles. Third, and most importantly, both the polarizabilities and all the multipoles are determined for each conformation of the protein by residue-wise QM calculations of the whole protein, ensuring that the conformational dependence of the polarizabilities and multipoles is explicitly accounted for. This conformational dependence has been shown to be significant, leading to errors of 3−43 kJ/mol for the electrostatic interaction energy between ligands and a protein or water solution.[52−55] Fourth, a large QM system is employed, 165−271 atoms, which ensures that the most important short-range interactions between the ligand and the protein are explicitly treated by QM, e.g., exchange, dispersion, charge transfer, charge penetration, as well as cross-terms and coupling to electrostatics and polarization. Fifth, a higher level of QM theory is employed than normally is used, MP2/cc-pVTZ. On the other hand, no geometry optimization at the PMISP/MM level is performed, and a fragmentation scheme is used to make the QM calculations feasible.

Solvation Calculations with the PCM Method. To accurately estimate ligand-binding affinities, an accurate estimate of the change in solvation energy upon ligand binding is needed. The standard continuum solvation methods for MM/PBSA in the AMBER software,[56] the Poisson−Boltzmann or generalized Born methods, cannot handle a multipole expansion or polarizabilities. Therefore, we instead decided to use the PCM method, which has recently been extended to be used with the effective fragment potential method (which also uses a polarizable force field with a multipole expansion).[57] We used the integral-equation formulation of PCM, IEFPCM,[58] which exhibits a better numerical stability than other formulations of PCM, and it is the default PCM method in the Gaussian software.[59] Owing to the large size of the molecular systems, the PCM-induced charges were obtained using a direct inversion of the iterative subspace procedure,[60] as implemented in the GAMESS software.[61] Thus, no explicit matrix inversion is needed. The PCM calculations were performed at the MM level, using the same multipoles and polarizabilities as in the PMISP calculations.

Like all continuum-solvation approaches, PCM employs dielectric cavities defined by a set of atomic radii. For accurate predictions of solvation energies, it is mandatory to use optimized cavity parameters. Several such sets of parameters are available for PCM at various levels of theory, e.g., Hartree−Fock[62] and density functional theory (UAHF and UAKS, i.e., united-atom topological model for Hartree−Fock and Kohn−Sham theory). Since we base our predictions on B3LYP and MP2 calculations, we decided to use the latter radii, which were optimized using the PBE0 functional.

Table 1. Calibration of the PCM Method for PMISP[a]

	scaling factor of radii for polar term												
	1.20	1.19	1.18	1.17	1.16	1.15	1.14	1.13	1.12	1.11	1.10	ΔG_{np}	exp.
H_2O	7.9	7.1	6.1	5.2	4.1	3.1	1.9	0.7	−0.5	−1.9	−3.3	6.3	−26.4[b]
CH_3OH	9.8	9.1	8.3	7.5	6.6	5.7	4.7	3.6	2.5	1.3	0.0	7.4	−21.4[b]
ethanol	10.7	9.9	9.1	8.3	7.3	6.4	5.4	4.2	3.0	1.7	0.4	8.2	−21.0[b]
p-$CH_3C_6H_4OH$	9.9	8.8	7.7	6.5	5.2	3.9	2.4	0.9	−0.8	−2.6	−4.6	10.0	−25.7[b]
NH_3	8.4	7.9	7.3	6.7	6.1	5.4	4.7	4.0	3.2	2.3	1.5	6.5	−17.9[b]
CH_3NH_2	11.7	11.1	10.5	9.8	9.1	8.3	7.5	6.6	5.7	4.7	3.6	7.5	−19.1[b]
CH_3CONH_2	13.7	12.6	11.5	10.3	9.0	7.6	6.2	4.7	3.2	1.6	−0.2	8.3	−40.6[b]
propionamide	15.2	14.2	13.1	11.9	10.7	9.4	8.0	6.5	5.0	3.4	1.7	8.9	−39.2[b]
CH_4	−1.4	−1.4	−1.4	−1.4	−1.4	−1.4	−1.5	−1.5	−1.5	−1.6	−1.6	7.1	8.4[b]
propane	0.1	0.1	0.1	0.0	0.0	0.0	0.0	−0.1	−0.1	−0.2	−0.2	8.5	8.2[b]
n-butane	0.3	0.3	0.3	0.3	0.3	0.2	0.2	0.2	0.1	0.1	0.0	9.3	8.7[b]
isobutane	−0.9	−0.9	−1.0	−1.0	−1.0	−1.1	−1.1	−1.1	−1.2	−1.2	−1.3	9.1	9.7[b]
toluene	5.9	5.5	5.2	4.8	4.4	4.0	3.5	3.0	2.5	1.9	1.3	9.6	−3.7[b]
CH_3SH	5.1	4.8	4.5	4.1	3.8	3.4	3.0	2.6	2.1	1.6	1.1	7.9	−5.2[b]
$CH_3SC_2H_5$	7.3	7.0	6.7	6.3	6.0	5.6	5.2	4.7	4.2	3.7	3.2	9.3	−6.2[c]
3-methylindol	8.2	7.1	6.0	4.8	3.6	2.3	0.9	−0.6	−2.2	−3.9	−5.7	10.7	−24.6[c]
4-methylimidazole	12.4	10.9	9.4	7.8	6.2	4.4	2.5	0.5	−1.6	−3.8	−6.3	9.1	−43.0[c]
N-propyl guanidine	17.3	15.5	13.7	11.7	9.6	7.4	5.0	2.5	−0.3	−3.3	−6.4	10.2	−45.7[d]
$CH_3NH_3^+$	36.8	34.2	31.6	28.9	26.1	23.3	20.4	17.4	14.4	11.3	8.1	7.8	−319.7[e]
imidazoleH$^+$	−9.2	−12.0	−14.8	−17.8	−20.9	−24.0	−27.3	−30.8	−34.3	−38.1	−42.0	8.5	−248.9[f]
$HCOO^-$	15.3	12.6	9.9	7.2	4.3	1.4	−1.6	−4.7	−7.9	−11.2	−14.6	7.2	−318.8[e]
CH_3COO^-	21.6	19.0	16.3	13.5	10.7	7.8	4.9	2.0	−1.0	−4.1	−7.3	8.1	−324.7[e]
MAD, all	10.4	9.6	8.8	8.0	7.1	6.2	5.4	4.7	4.4	4.8	5.2		
MAD, neutral	8.1	7.5	6.8	6.0	5.2	4.4	3.5	2.7	2.2	2.3	2.3		

[a] The total solvation free energies of 22 organic molecules and ions were calculated with the PCM+SASA method, using different values for the scaling factor of the radii for the electrostatic term (1.10−1.20). The SASA nonpolar energy, calculated with Parse radii,[67] was added to these values, and the results were compared to experiments. In the table, the differences compared to experiments are given, as well as the nonpolar energy term (ΔG_{np}) and the experimental data (exp.)[64−68] (all in kJ/mol). [b] Data from ref 64. [c] Data from ref 66. [d] Data from ref 67. [e] Data from ref 65. [f] 18.8 kJ/mol was added to the value in ref 68 to use the same value of the absolute solvation energy of a proton as in ref 65.

These radii, although not yet properly published, are available in the Gaussian 03 suite of programs.[63]

Since we use the UAKS parameters at the MM level, recalibration of these parameters is strictly needed. However, we limited the recalibration to a scaling of the radii for the electrostatic component in the PCM solvation energy calculation. For the original UAKS radii, this scaling parameter is 1.2. The calibration was based on a test-set of 22 small organic molecules, listed in Table 1. These molecules were selected to represent models of the peptide backbone and all amino acid side chains. For these, we constructed distributed multipoles up to quadrupoles and anisotropic polarizabilities in the same way as for PMISP.[9] The multipoles and polarizabilities were calculated using the B3LYP/6-31G* method (6-31+G* for the two anions), and the solvation energies were then evaluated using the PCM approach for various values of the scaling parameter. The nonpolar solvation terms (cavitation, dispersion, and exchange repulsion[62]) are independent of this scaling factor and were therefore calculated only once. As will be discussed below, we encountered serious problems with the nonpolar terms in the PCM model. Therefore, the final calibration of the PCM method (Table 1) employed instead the nonpolar energy from the standard MM/PBSA method. A fitting to experimental data[64−68] gave a scaling factor of 1.12 (with the nonpolar terms from PCM, the optimum scaling factor was 1.15). This decrease in the scaling factor is expected, because there is no charge penetration at the MM level. The scaled model gave MADs of 2 and 4 kJ/mol, for the neutral molecules and all molecules, respectively. This is only slightly worse than for the UAHF parameters (1 and 3 kJ/mol), similar to the UAKS parameters (1 and 5 kJ/mol), and appreciably better than seven different Poisson−Boltzmann and 11 generalized Born methods (3−9 and 7−18 kJ/mol).[69] For the seven biotin analogues, this recalibrated PCM method gives a MAD of 10 kJ/mol, compared to a weighted average of 24 different continuum solvation methods,[69] which again is slightly worse than for the original UAHF and UAKS methods (4 and 7 kJ/mol).

MM/PBSA. The calculations in this paper are based on the MM/PBSA approach.[7] We selected the MM/PBSA approach because it is widely used and has been shown to give reasonable results for many systems.[7,35,38,39,70−72] It also contains no adjustable parameters and has a modular approach with separate energy terms, which facilitates the incorporation of QM data. However, we do not claim that this approach is more accurate or effective than other approaches.

In this method, the binding affinity (the free energy of the reaction in eq 1, ΔG_{bind}) is estimated from the free energies of the three reactants,

$$\Delta G_{bind} = G(\mathrm{PL}) - G(\mathrm{P}) - G(\mathrm{L}) \qquad (5)$$

where all species are assumed to be in water solution. The free energy of each of the reactants is estimated as a sum of four terms:

$$G = \langle E_{MM} \rangle + \langle G_{solv} \rangle + \langle G_{np} \rangle - T\langle S_{MM} \rangle \qquad (6)$$

where G_{solv} is the polar solvation energy of the molecule, estimated by the solution of the Poisson−Boltzmann (PB) equation,[73] G_{np} is the nonpolar solvation energy, estimated

from the solvent-accessible surface area (SASA) of the molecule,[74] T is the temperature, S_{MM} is the entropy of the molecule, estimated from a normal-mode analysis of harmonic frequencies calculated at the molecular mechanics (MM) level, and E_{MM} is the MM energy of the molecule, i.e., the sum of the internal energy of the molecule (i.e., bonded terms, E_{bond}), the electrostatics (E_{es}), induction energy (E_{ind}, only if a polarizable force field is used), and van der Waals interactions (E_{vdW}):

$$E_{MM} = E_{bond} + E_{es} + E_{ind} + E_{vdW} \quad (7)$$

All of the terms in eq 6 are averages of energies obtained from a number of snapshots taken from MD simulations. To reduce the time-consumption and increase the precision, the same geometry is normally used for all three reactants (complex, ligand, and receptor); i.e., only the PL complex is explicitly simulated by MD.[75] Thereby, E_{bond} cancels in the calculation of ΔG_{bind}.

In this investigation, we test if the binding-affinity predictions can be improved by replacing some of these terms with estimates using other methods. Thus, we replace the E_{MM} term by the PMISP/MM interaction energy between the ligand and the protein (eq 6). Second, we replace the $G_{solv} + G_{np}$ estimates of the solvation energies by the corresponding terms within the PCM model. The E_{ind} and G_{solv} terms are computed in a self-consistent way, as described in ref 57 and implemented in GAMESS.[61] Thus, the apparent surface charges and the induced dipoles are simultaneously iterated to self-consistency. Then, E_{ind} is defined as the energy of the induced dipoles in the electric field of the multipoles and G_{solv} as the energy of the apparent surface charges in the electric potential of the multipoles, with both terms divided by two to account for the self-energy of polarization. This decomposition is only used in the qualitative discussion; only the sum of these terms is well-defined and influences the result. Other approaches to replace the E_{MM} term with a standard QM/MM term have been tested, both for calculations of ligand-binding affinities and for other energies.[76−78] A possible problem, common to these methods and to PMISP/MM/PCM, is that the geometries are not generated by the same energy function as used to evaluate the binding affinities. However, it should be noted that a similar problem exists for the original MM/PBSA method when the geometries are generated using explicit solvent, but the energies are calculated with implicit solvent. Moreover, this problem is reduced by using multiple snapshots instead of a single minimized structure.

Thus, only the S_{MM} term is kept from the original MM/PBSA method, but it is calculated according to our recently developed method to improve the precision of this estimate.[79] In the original approach,[7] the protein was truncated 8 Å from the ligand, and it was then freely optimized, using a distance-dependent dielectric constant $\varepsilon = 4r$. We have shown that this gives a large statistical uncertainty in the entropy estimate, which can be reduced by a factor of 2−4 if a buffer region of 4 Å is used outside the cutoff radius. This buffer region is kept fixed in the geometry optimization and is not included in the estimate of the entropy, but it ensures that the optimized system stays close to the structure in the complex. This also makes the use of the questionable distance-dependent dielectric constant superfluous.

The results of the PMISP/MM/PCM/$T\Delta S$ approach are compared to the results of standard MM/PBSA calculations using the polarizable Amber 2002 force field.[45] These were performed in the same way as in our previous investigation of various force fields for the biotin−avidin system[38] (the 02ohp/02 calculations in that work, although the present calculations are based on the ligand in the fourth subunit in the tetramer, rather than the first one in the previous investigation). This means that G_{solv} is estimated by adding an extra charge close to each atom site to simulate the induced dipoles in the PB calculations. Calculations of both G_{solv} and G_{np} used Parse radii.[67] The calculations were performed with the Amber software,[56] but with the improved entropy estimate[79] (this term is identical to the one used in the PMISP/MM/PCM/$T\Delta S$ approach). Unfortunately, the Amber nmode program does not work properly for a polarizable force field, so the entropy calculations were performed without the polarizabilities.

AutoDock Calculations. Standard docking calculations were performed with AutoDock 4.[80] Three sets of calculations were performed. In the first set, we simply rescored the same snapshots used in the MM/PBSA calculations with the AutoDock scoring function[81] and averaged the results. In the second set, we docked the ligand into the equilibrated protein structure for each ligand, as represented by the first snapshot from the MD simulations. Finally, in the third set, we docked the ligand into the crystal structure. In addition, we tested the influence of the partial charges by performing all calculations with either the default (Gasteiger) charges or the Amber charges used in the MD simulations. Default settings (e.g., atom types) were used. The protein was considered rigid in all docking calculations, whereas the ligands were fully flexible.

Studied Systems. We studied the binding of the seven biotin analogues (BTN1−BTN7) in Figure 1 to avidin. The setup of the molecular dynamics simulations has been described before.[38] We used 10 snapshots (sampled every 20 ps) for each analogue taken from this investigation, performed by the polarizable Amber 2002 force field[45] (the 02ohp simulation in ref 38). Error estimates of the correlation coefficients and the mean absolute deviations were obtained by 10 000 random simulations, as has been described before.[39] It is likely that the reported standard deviations are underestimates because the structures come from a single simulation, rather than several independent simulations.[39]

Timings. A single-point calculation with the PMISP/MM/PCM/$T\Delta S$ method took 38−45 CPU days. Most of this time was spent on the property calculations (∼30 CPU days), which could be significantly sped up by using software optimized for density functional theory. The supermolecular calculations took 5−12 CPU days depending on the ligand size and the PCM calculations took 3 CPU days, whereas the computational time for all other steps was negligible. All calculations were run trivially in parallel. The corresponding time for a single-point MM/PBSA evaluation is less than 1 CPU hour. However, in that case, the computa-

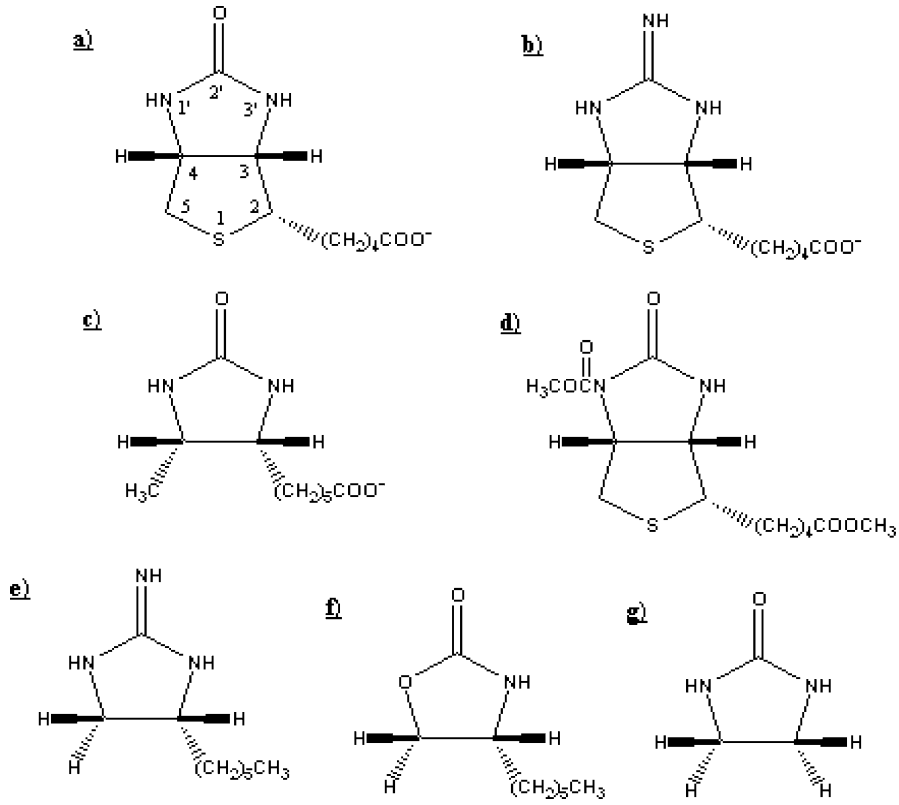

Figure 1. The seven biotin analogues used in this study. (a) BTN1 (biotin), (b−g) BTN2−BTN7.

Table 2. Average Nonpolar Solvation Energies (kJ/mol) in the SASA and PCM Calculations[a]

	SASA				PCM						
	PL	P	L	PL−P−L	PL	P	L	PL−P−L	cav	disp	rep
BTN1	464.5	466.9	14.1	−16.5	22282.5	22156.3	12.3	113.9	−18.5	189.5	−57.2
BTN2	466.1	468.8	14.1	−16.8	22274.8	22144.1	14.4	116.3	−19.8	197.6	−61.4
BTN3	471.5	474.1	14.1	−16.7	22234.1	22116.7	6.7	110.7	−21.6	180.8	−48.5
BTN4	468.7	472.9	16.3	−20.5	22447.5	22267.7	24.4	155.4	−22.4	236.2	−58.5
BTN5	465.5	468.1	13.4	−16.0	22250.3	22137.8	8.0	104.5	−18.2	163.5	−40.9
BTN6	466.7	469.6	13.1	−16.0	22228.3	22119.1	8.9	100.5	−19.1	153.4	−33.9
BTN7	478.4	479.8	9.3	−10.6	21941.9	21892.2	−2.5	52.3	−7.5	89.1	−29.3

[a] The energy contributions for the complex (PL), protein (P), and ligand (L) given, as well as the net contribution to the binding (PL−P−L), for PCM further divided into cavitation (cav), dispersion (disp), and repulsion (rep) contributions.

tional time is dominated by the generation of snapshots, which took 7 CPU days per ligand.[38]

Result and Discussion

Nonpolar Solvation Energy. First, we calculated the solvation energies using the full PCM model implemented in the GAMESS program.[61] However, this gave differential solvation energies (i.e., $G_{solv}(PL) + G_{np}(PL) - G_{solv}(P) - G_{np}(P) - G_{solv}(L) - G_{np}(L)$) that were 60−180 kJ/mol more positive than the corresponding results with a PB+SASA model. Further inspection showed that these differences arise almost entirely from the nonpolar part of the solvation energy: In the PB+SASA method, this term is taken from the difference in the solvent-exposed surface area between the complex and the isolated protein and ligand. From the results presented in Table 2, it can be seen that the SASA nonpolar energies are quite small and similar for the complex and the protein, ∼470 kJ/mol (corresponding to a SASA of 20 600 Å^2, because ΔG_{np} = SASA × 0.0227 − 3.85 kJ/mol, when SASA is given in Å^2 [7,35,38]). The difference is 1−4 kJ/mol, with the protein having the largest value, indicating that the ligand is mainly buried in the protein. Therefore, the net nonpolar SASA effect comes mostly from the ligand. As an effect, ΔG_{np} in MM/PBSA is small and negative for all complexes, 11−21 kJ/mol, and directly related to the size of the ligand.

However, in the PCM method, the nonpolar solvation energy is calculated from three separate terms: the energy cost of making a cavity in the solvent (the cavitation energy), a favorable term from the dispersion interactions between the solute and the solvent, and the corresponding unfavorable term from exchange repulsion.[62] The former term is calculated from an expression that contains terms involving the radius of each atom to the power of 0, 1, 2, and 3,[82−85] i.e., including a term that is proportional to the volume, whereas the latter two terms are calculated by a surface-based integration method.[86] From Table 2, it can be seen that the PCM energies of the protein and the complex are almost 50

times larger than the SASA energies, ~22 200 kJ/mol. The PCM energies are dominated by the cavitation energy, which is ~28 000 kJ/mol, compared to the dispersion energy of ~−7500 kJ/mol and the exchange repulsion energy of ~2000 kJ/mol. However, when computing the difference upon binding, the cavitation energy is mainly canceled (the net effect is negative and 8−22 kJ/mol; cf. Table 2). This indicates that the volume term of the cavitation energy is dominating the individual energies, because the volume hardly changes during ligand binding. On the other hand, the surface area is reduced, and this causes a positive (unfavorable) contribution from the dispersion term of 89−236 kJ/mol, only partly canceled by the exchange repulsion (negative and 29−61 kJ/mol) and by the small cavitation energy. Therefore, the net ΔG_{np} is 52−155 kJ/mol; i.e., it has the opposite sign and is larger in magnitude compared to the SASA nonpolar solvation energy. It is notable that the two methods are reasonably in accord for the ligand: The SASA energy estimate is 9−16 kJ/mol (corresponding to SASAs of 240−550 Å^2), whereas the PCM nonpolar energies are −3 to +24 kJ/mol with a correlation coefficient $r^2 = 0.85$.

This illustrates a major problem in estimating binding affinities using approaches that involve a continuum estimate of the solvation energy. Apparently, there is no consensus as to how the nonpolar energy should be estimated, and the PCM and SASA approaches give strongly differing results. It has previously been argued that it does not matter whether the area or volume is used to estimate the nonpolar solvation energy.[87] However, the present results show that this is not the case for ligand-binding affinities: When a ligand binds to a complex, the volume of the protein increases approximately by the volume of the ligand (so that the total volume during the binding reaction hardly changes). However, the SASA typically decreases during the binding, because the ligand becomes partly hidden by the protein and an empty cavity in the protein becomes filled by the ligand. In PCM, this is further complicated by the use of several energy terms with different functional forms. In fact, it appears that the cavity term (after cancellation of the volume contributions) contains the same information as the SASA estimate (the difference is always within 5 kJ/mol). The additional terms used in PCM (dispersion and repulsion) do not appear to give any advantage for protein−ligand energies; on the contrary, the results deteriorate. It should be noted that these terms are well motivated from a physical point of view and, for example, that the three-dimensional reference interaction site model (3D-RISM[88,89]) gives nonpolar energies of the same size and sign as PCM.[90] Therefore, this seems to be a parametrization problem, possibly related to the general difficulty of using terms with different signs in a fitting expression. However, we cannot exclude the possibility that the better result for the SASA estimate is fortuitous. We currently investigate this issue for other systems.

Another difference between the two solvation methods is that the PB method is based on the SASA, whereas the cavitation terms in PCM are based on the van der Waals surface of the solute (and the other terms on the solvent-excluded surface area, SESA).[91] The van der Waals surface is simply the surface of the union of spheres on all atoms with the corresponding van der Waals radius, whereas the SASA is the surface defined by the center of a spherical solvent probe that is rolled on the van der Waals surface. Therefore, the radius of a solvent molecule (~1.4 Å for water) is added to the van der Waals radii of each atom, and crevices between the spheres that are not accessible to a solvent probe are considered as a part of the solute. The SESA is similar to the van der Waals surface, but it excludes those crevices. For small molecules, for which the PCM method was calibrated,[62] these three surfaces are rather similar. However, for a large molecule, like a protein, they are totally different, because there are numerous small cavities inside the protein that are not large enough to house a solvent probe. The solvent-accessible surface of the protein will essentially be only the outer surface of the protein, whereas the van der Waals surface will be much larger. For example, for the avidin tetramer, the van der Waals area is 58 000 Å^2, and all atoms contribute to it, whereas the SASA is only 21 000 Å^2, and only 40% of the atoms contribute to it. The SESA is ~20 000 Å^3. It should be noted that this effect becomes apparent already for much smaller molecules. For example, in our study of solvation energies of drug-like molecules, the PCM estimates differed by 100−150 kJ/mol from that of all other methods for the two largest molecules (with 68 and 113 atoms).[69]

It seems quite questionable to use the van der Waals surface to calculate the solvation energy of a protein. Therefore, we tend to prefer the SASA model, which also gives 50 times smaller energies and thus probably more precise differences. We have therefore based the recalibrated PCM model on the nonpolar SASA energies. We do not argue that this is an optimum approach—on the contrary, it would be better to develop a new PCM method that works properly also for a protein, based on the SASA or SESA. Unfortunately, this is a major task, involving both method development and a complete reparametrization of the method so that it works well both for small molecules and for proteins. Moreover, it has to be settled whether the nonpolar term should be based on the volume or the surface area. This is out of the scope of the present investigation.

Binding Affinity Estimates. Table 3 shows the various terms in the full PMISP/MM/PCM/$T\Delta S$ method (with the nonpolar solvation energies from the PCM method; column ΔG_1). It can be seen that the method gives poor absolute affinities, ranging from +30 to +103 kJ/mol, compared to the experimental data, −19 to −85 kJ/mol (Figure 2),[30−32] with a mean absolute deviation from the experimental values (MAD) of 108 kJ/mol. If we allow for a systematic error in the method (i.e., if we translate all points with the mean signed error), we still get a mean absolute deviation (TR MAD) of 19 ± 3 kJ/mol, with the largest error for BTN1. This result is disappointing. It is worse than similar MM/PBSA calculations using various MM force fields for the same system, which gave MADs of 9−19 kJ/mol, and TR MADs of 5−19 kJ/mol.[38] In particular, the standard MM/PBSA calculations for exactly the same snapshots, using the Amber 2002 force field, give a MAD and TR MAD of 13

Table 3. Results of the PMISP/MM/PCM/$T\Delta S$ Method (kJ/mol)[a]

exp	ΔE_{es}	ΔE_{ind}	ΔE_{nc}	$\Delta G_{solv,PCM}$	$\Delta G_{np,PCM}$	$-T\Delta S$	$\Delta G_{np,SASA}$	ΔE_{vdW}	ΔE_{coop}	ΔG_1	ΔG_2	ΔG_3
BTN1	−1061.2	−253.5	−75.0	1236.5	113.9	96.8	−16.9	−143.4	78.9	57.6	−73.1	−141.6
BTN2	−1109.5	−322.7	−67.5	1311.3	116.3	102.4	−17.2	−149.1	94.3	30.4	−103.2	−184.8
BTN3	−1055.0	−282.3	−61.9	1235.0	110.7	93.4	−16.7	−138.6	95.7	39.9	−87.5	−164.1
BTN4	−123.1	−55.9	−151.1	181.1	155.4	96.5	−21.3	−211.0	−0.5	103.0	−73.6	−133.5
BTN5	−112.6	−50.9	−92.4	140.7	104.5	77.4	−16.2	−134.5	−10.3	66.7	−54.0	−96.1
BTN6	−88.5	−45.3	−91.0	132.9	100.4	69.8	−15.8	−131.9	−5.3	78.4	−37.8	−78.8
BTN7	−112.5	−46.3	−22.6	127.4	52.3	66.4	−10.7	−53.6	−14.1	64.6	1.7	−29.3
MAD										107.9	25.5	73.4
TR MAD										19.2	18.6	30.6
R^2										0.27	0.52	0.59

[a] Three different estimates of the total binding energy are given: $\Delta G_1 = \Delta E_{es} + \Delta E_{ind} + \Delta E_{nc} + \Delta G_{solv,PCM} + \Delta G_{np,PCM} - T\Delta S$ is the full PMISP/MM/PCM/TΔS, whereas in $\Delta G_2 = \Delta E_{es} + \Delta E_{ind} + \Delta E_{nc} + \Delta G_{solv,PCM} + \Delta G_{np,SASA} - T\Delta S$, the nonpolar PCM term has been replaced by the nonpolar SASA term, and in $\Delta G_3 = \Delta E_{es} + \Delta E_{ind} + \Delta E_{vdW} + \Delta G_{solv,PCM} + \Delta G_{np,SASA} - T\Delta S$, the ΔE_{nc} term has also been replaced by the Amber van der Waals energy. The mean absolute deviation (MAD), the correlation coefficient (R^2), as well as the MAD after subtraction of the mean signed deviation (TR MAD) are also given for each energy estimate. ΔE_{coop} is the cooperativity of the binding in a vacuum, defined as the difference between the induction energy of the whole protein−ligand complex and the sum of pairwise induction energies for the fragment−ligand dimers.

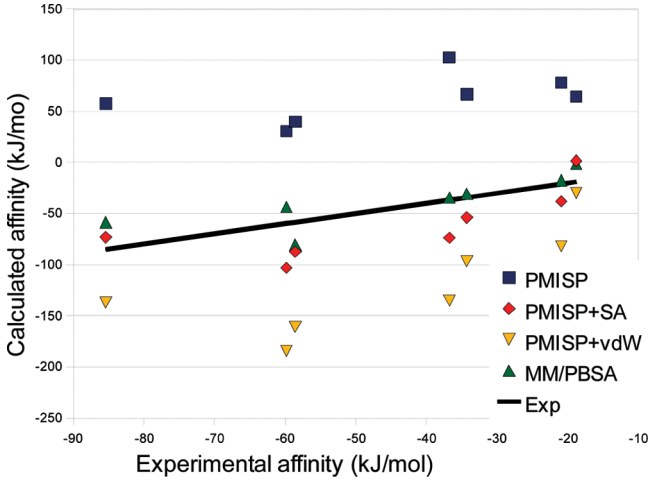

Figure 2. The results of the PMISP/MM/PCM/$T\Delta S$, PMISP/MM/PCM/SASA/$T\Delta S$, PMISP/MM/PCM/SASA/$T\Delta S/E_{vdW}$, and MM/PBSA (with the Amber-02 force field) methods for the binding of seven biotin analogues to avidin.

and 11 ± 3 kJ/mol (Table 4), respectively. In fact, the result is not significantly better than assigning the same affinity to all seven biotin analogues, which gives a TR MAD of 20 kJ/mol. The correlation coefficient is also poor, $R^2 = 0.27 \pm 0.10$, compared to 0.65 ± 0.09 for MM/PBSA and 0.43−0.98 in our previous investigation.[38]

The replacement of the PCM nonpolar term by the SASA term (as discussed above) gave the same TR MAD, although the binding affinities are shifted to a range that is closer to the experimental one, +2 to −103 kJ/mol (column ΔG_2 in Table 3), and the correlation coefficient is improved ($R^2 = 0.52 \pm 0.09$). If the nonpolar solvation energy is omitted, the result is improved in absolute terms, so that both the MAD and TR MAD are 17 ± 2 kJ/mol, but R^2 remains similar, 0.55 ± 0.10.

The standard deviations of the various PMISP/MM/PCM/$T\Delta S_{MM}$ energy terms are listed in Table 5. It can be seen that they are 10−30 kJ/mol for the final binding energy. Thus, the standard errors of the mean values are 3−9 kJ/mol, showing that the statistical precision cannot explain the poor results. The standard deviation is dominated by the electrostatics, induction, polar solvation, and nonclassical terms, which typically give slightly larger standard deviations than the total energy, because some of the variation between these terms is canceled. The standard deviation of the entropy term is also quite large, 9−21 kJ/mol, but it never limits the precision of the method. The standard deviation of the nonpolar solvation energy is always less than 1 kJ/mol. The corresponding standard deviations for the MM/PBSA method are also listed in Table 5. The standard deviations of the electrostatics and entropy terms are similar to that for PMISP, but those of the solvation and the nonclassical terms are somewhat smaller.

To see how these results compare with other simpler methods, we tried to correlate the binding affinities to the molecular weight of the ligands or to the Amber van der Waals term alone. However, this gave poor correlations to the experimental data, $R^2 = 0.20$ and 0.11, respectively.

Next, we performed a docking study of the same ligands using AutoDock.[80] The results are shown in Table 6. First, we rescored the MD snapshots used in the MM/PBSA calculations with the AutoDock scoring function.[81] This gave good agreement with the experimental values for the neutral ligands, whereas the binding free energies of the charged ligands were too positive. Nevertheless, the MAD with Gasteiger charges was 16 kJ/mol, and the TR MAD was 13 kJ/mol. The Amber charges gave consistently less negative binding affinities and thus a larger MAD (30 kJ/mol), but the relative energies were not significantly affected (TR MAD 14 kJ/mol). Interestingly, the standard deviations over the snapshots, listed in Table 5, were significantly smaller than for the PMISP or MM/PBSA calculations, ranging from 1 to 4 kJ/mol for the various ligands.

Next, we docked the ligand into the equilibrated protein structure. This gave similar results (TR MADs of 13−14 kJ/mol), because the best docked binding pose agreed with the one used in the MD simulations (average root-mean-squared deviation in geometries of 0.8 Å) in all cases except one (BTN5 with Amber charges). On average, the binding free energy was 2 kJ/mol more favorable when the ligand was allowed to relax.

Finally, we docked the ligand into the crystal structure. Again, the best docked binding mode agreed with the one

Table 4. Results for the MM/PBSA Calculations Using the Polarizable Amber 2002 Force Field (kJ/mol)[a]

	ΔE_{es}	ΔE_{ind}	ΔE_{vdW}	$\Delta G_{solv,PB}$	$\Delta G_{np,SASA}$	$-T\Delta S$	ΔG_{bind}	exp.
BTN1	−1173.6	−1.6	−143.4	1180.0	−16.9	96.8	−58.6	−85.4
BTN2	−1213.8	14.6	−149.2	1220.0	−17.2	102.4	−43.2	−59.8
BTN3	−1182.2	−0.6	−138.6	1164.1	−16.7	93.4	−80.6	−58.6
BTN4	−127.0	−14.6	−211.0	243.1	−21.3	96.6	−34.2	−36.8
BTN5	−100.7	−16.3	−134.5	159.4	−16.1	77.4	−30.9	−34.3
BTN6	−80.4	−11.2	−131.9	152.1	−15.8	69.8	−17.4	−20.9
BTN7	−111.4	−9.6	−53.6	117.6	−10.6	66.4	−1.2	−18.8

[a] The MAD and TR MAD are 13.2 and 11.5 kJ/mol, respectively, and R^2 is 0.65.

Table 5. Standard Deviations of the Various Terms for PMISP/MM/PCM/$T\Delta S_{MM,}$ MM/PBSA, and AutoDock with Gasteiger (G) and Amber (A) Charges (kJ/mol)[a]

	MM/PBSA								PMISP/MM/PCM/$T\Delta S$							G	A
	E_{es}	E_{ind}	E_{vdW}	G_{PB}	G_{SASA}	$T\Delta S$	G_{bind}	E_{eis}	E_{es}	E_{ind}	E_{nc}	G_{PCM}	$G_{np,PCM}$	G_{bind}	E_{eis}	G_{bind}	G_{bind}
BTN1	20.9	5.4	15.0	18.8	0.2	14.2	18.7	19.6	17.6	17.6	25.8	22.0	0.2	23.4	18.4	1.4	1.4
BTN2	37.6	4.6	14.4	21.0	0.2	21.0	25.4	25.5	32.0	32.2	23.3	45.4	0.2	26.3	33.9	2.7	3.0
BTN3	26.0	6.8	11.6	17.9	0.2	11.7	22.1	29.3	25.1	24.2	31.0	24.8	0.2	14.7	29.6	3.4	3.2
BTN4	15.5	3.8	10.8	16.5	0.3	11.8	20.7	19.8	18.8	9.8	14.1	11.9	0.3	16.9	19.9	3.6	3.4
BTN5	18.9	3.9	8.0	16.7	0.1	12.1	21.8	23.6	13.3	13.3	13.9	15.8	0.1	9.8	14.6	1.2	1.4
BTN6	15.1	3.1	15.3	8.7	0.2	15.3	21.1	17.4	13.1	11.0	19.9	15.4	0.2	14.9	14.0	2.0	1.8
BTN7	10.6	3.1	7.8	10.9	0.1	9.3	18.5	16.6	11.6	6.9	13.2	8.4	0.1	9.9	12.5	1.1	1.2

[a] E_{eis} is the sum of the E_{es}, E_{ind}, and G_{solv} terms.

Table 6. Binding Free Energies (kJ/mol) Obtained from the AutoDock Calculations Based on Rescoring of the MD Snapshots, Docking into Snapshot 1, or Docking into the Crystal Structure, Using Gasteiger or Amber Charges

	rescoring		docking (snapshot)		docking (crystal)	
	Gasteiger	Amber	Gasteiger	Amber	Gasteiger	Amber
BTN1	−37	−24	−40	−26	−38	−27
BTN2	−37	−23	−41	−24	−36	−25
BTN3	−36	−19	−37	−21	−35	−20
BTN4	−35	−15	−37	−17	−33[a]	−11[a]
BTN5	−21	−7	−22	−7[a]	−21[b]	−19[b]
BTN6	−22	−10	−26	−13	−27[a]	−9[b]
BTN7	−14	−8	−15	−8	−13[b]	−9[a]
MAD	16	30	15	28	18	28
TR MAD	13	14	13	14	13	14
R^2	0.68	0.83	0.66	0.79	0.65	0.84
slope	0.32	0.27	0.33	0.28	0.31	0.29

[a] Simulated pose not found. [b] Simulated pose ranked 2nd or 3rd.

used in the MD simulations for all the charged ligands. For the other ligands, the simulated pose was sometimes ranked second and third (with differences of ∼1 kJ/mol), whereas in some cases, the simulated pose was not among the docked binding poses (see Table 6). This probably reflects the fact that the crystal structure was obtained using biotin (BTN1), and thus a rigid protein represents a crude approximation when the ligands differ significantly in size. Reassuringly, the predicted binding free energies from the crystal docking were always similar or slightly larger (up to 6 kJ/mol) than that found in the docking to the MD snapshots (with the same exception as before, BTN5 with Amber charges). This indicates that the simulated pose is the correct one for all ligands. The TR MADs from the crystal docking were again 13−14 kJ/mol.

The correlation coefficients for the AutoDock results (R^2) ranged from 0.65 to 0.83. However, the slopes of the correlation lines are small (0.24−0.33), indicating that the energy scale of the AutoDock scoring function is less quantitative than the methods based on PMISP (which give slopes of 0.5−2.2). Overall, the AutoDock results are similar or sometimes slightly better than those based on PMISP. An important reason for this is the smaller standard deviation of the AutoDock results. A more physical energy function will give energy terms that are larger in magnitude, but to a large extent canceling. Thus, it needs to have a much higher accuracy than a less detailed model to give a better final result. In fact, many energy functions can be improved by simply scaling down all terms. For example, if ΔG_2 in Table 3 (PMISP/MM with SASA) is scaled down by a factor 2, the MAD and TR MAD become 14 and 11 kJ/mol (whereas R^2 does not change from 0.52), respectively, but at the same time, the slope of the correlation line is reduced from 1 to 0.5.

We will try to rationalize the failure of PMISP by analyzing the various terms in the method in comparison to MM/PBSA. The entropy term is identical between the two methods, and the nonpolar solvation term is also identical in the ΔG_2 estimate, so these cannot explain the failure.

The polar solvation energies show differences of −62 to +91 kJ/mol (PMISP/MM/PCM is mostly more negative for the neutral ligands and always more positive for the charged

ligands). However, the correlation is excellent for the neutral ligands, $R^2 = 0.97$, and rather good for the charged ones, $R^2 = 0.93$.

The electrostatic and induction energies of the PMISP and MM/PBSA methods are not comparable, because intramolecular induction is not treated in the same way.[9] Therefore, we can only compare the sum of these two terms. It turns out that this sum is always more negative with PMISP than with MM/PBSA, by 37−47 kJ/mol for the neutral ligands, and by 140−233 kJ/mol for the charged ligands. However, again, the two terms are almost perfectly correlated, with an R^2 of 0.98 and 0.96 for the charged and neutral ligands, respectively.

If the solvation energy is added to this sum, the difference is partially canceled, but the PMISP/MM/PCM results are still 28−142 kJ/mol more negative than the MM/PBSA results. Interestingly, the good correlation is completely lost, especially for the charged ligands ($R^2 = 0.11$, versus 0.84 for the neutral ligands).

Finally, the nonclassical (van der Waals) energies also differ by a sizable but rather constant amount, 31−82 kJ/mol, which is slightly larger for the charged ligands than for the neutral ones. The PMISP estimates are always more positive. There is a perfect correlation ($R^2 = 1.00$) between Amber and PMISP for the neutral ligands, but it is much worse for the charged ones ($R^2 = 0.14$). If we replace the nonclassical PMISP term with the Amber van der Waals term, the results become worse, with a TR MAD of 31 kJ/mol (but R^2 increases to 0.59; cf. Figure 2).

Recently, it has been shown that there are strong cooperative effects in the binding of biotin to avidin (∼45 kJ/mol at the MP2/6-31+G** level).[92] Such effects are included in the present calculations through the polarizabilities. However, from the results in Table 3 (column ΔE_{coop}), it can be seen that we actually find strong anticooperative effects for the three charged ligands (by 79−96 kJ/mol for the full protein and 24−31 kJ/mol for the region *M*), whereas we find cooperative effects for the four neutral ligands (0−14 kJ/mol). The reason for this discrepancy is most likely that the previous calculations omitted the carboxylate tail of biotin and therefore its negative charge.

Conclusions

In this paper, we present the first attempt to calculate ligand-binding affinities using high-level QM methods with large basis sets (MP2/cc-pVTZ, i.e., enough to get reasonably accurate dispersion energies), combined with estimates of solvation energies, entropy, as well as sampling effects. To this aim, we have used the recently developed PMISP method, which has been calibrated and tested for the biotin−avidin complexes and has been shown to give protein−ligand interaction energies with an accuracy of 3−5 kJ/mol compared to full QM calculations with the same method.[9] We have also shown that the surrounding protein can be modeled by a PMISP/MM approach, and we have tested different sizes of the PMISP model.[25] In this paper, we have combined this method with the PCM solvation model, which has been used before to calculate ligand-binding affinities.[60] These methods are combined to evaluate binding affinities through the widely used MM/PBSA approach,[7] using a normal-mode estimate of the entropy change during ligand binding and sampling geometries from an MD simulation of the solvated complex.

Unfortunately, the results with this PMISP/MM/PCM/$T\Delta S$ approach are rather poor in both absolute and relative terms, with a TR MAD of 19 kJ/mol, i.e., worse than a standard MM/PBSA method for the same problem (11 kJ/mol) or docking results with AutoDock (13−14 kJ/mol). The reason for the poor absolute binding affinities is probably the contribution from the PCM nonpolar solvation energies, which is 60−180 kJ/mol more positive than that obtained with the simple SASA-based method in standard MM/PBSA. On the other hand, the relative energies are not much improved when the PCM nonpolar solvation energies are replaced by SASA-based estimates (TR MAD = 19 kJ/mol). In fact, the best results are obtained without any nonpolar terms at all (TR MAD = 17 kJ/mol). A possible problem with the present approach is that we calculate the PMISP energies on snapshots from a MD simulation performed with another energy function. It is conceivable that the mismatch between the two potential energy surfaces may give rise to sizable errors.[38]

The use of high-level QM interaction energies allows us to address the important question of whether the accuracy of the MM/PBSA method is limited by the accuracy of the force field. Clearly, our results indicate that this is not the case. However, we cannot say whether the limitation resides in the solvation model or in the statistical-mechanical approximations inherent in the method. For this, it would be necessary to have a solvation model that is specifically parametrized for the electrostatics corresponding to high-level QM calculations and that is consistent for both large and small systems, so that the solvation contribution to binding energies can be accurately calculated. In this study, we have pointed out several qualitative differences between the nonpolar part of the PCM model and the corresponding SASA estimate, thus providing a starting point for understanding how such an ideal method should behave. In particular, it must be settled what type of expression (volume and area terms in PCM, only area terms in SASA) is most transferable between various solute sizes and what type of solute surface (van der Waals surface in PCM, solvent-accessible surface area in SASA) is most easily parametrized. Intuitively, it seems questionable to use a surface (e.g., the van der Waals surface) that contains contributions for atoms deeply buried in the protein and gives rise to many cavities.

Acknowledgment. This investigation has been supported by grants from the Swedish research council and AstraZeneca, as well as by computer resources of Lunarc at Lund University. J.K. thanks the Villum Kann Rasmussen foundation and the Danish research council for financial support.

References

(1) Gohlke, H.; Klebe, G. *Angew. Chem., Int. Ed.* **2002**, *41*, 2644–2676.

(2) Beveridge, D. L.; Dicapua, F. M. *Annu. Rev. Biophys. Biophys. Chem.* **1989**, *18*, 431–492.

(3) Lee, F. S.; Chu, Z. T.; Bolger, M. B.; Warshel, A. *Protein Eng.* **1992**, *5*, 215–228.

(4) Sham, Y. Y.; Chu, Z. T.; Tao, H.; Warshel, A. *Proteins: Struct., Funct., Genet.* **2000**, *39*, 393–407.

(5) Warshel, A.; Sharma, P. K.; Kato, M.; Parson, W. W. *Biochim. Biophys. Acta* **2006**, *1764*, 1647–1676.

(6) Hansson, T.; Marelius, J.; Åqvist, J. *J. Comput.-Aided Mol. Des.* **1998**, *12*, 27–35.

(7) Kollman, P. A.; Massova, I.; Reyes, C.; Kuhn, B.; Huo, S.; Chong, L.; Lee, M.; Lee, T.; Duan, Y.; Wang, W.; Donini, O.; Cieplak, P.; Srinivasan, J.; Case, D. A.; Cheatham, T. E. *Acc. Chem. Res.* **2000**, *33*, 889–897.

(8) Pearlman, D. A.; Charifson, P. S. *J. Med. Chem.* **2001**, *44*, 3417–3423.

(9) Söderhjelm, P.; Ryde, U. *J. Phys. Chem. A* **2009**, *113*, 617–627.

(10) Khoruzhii, O.; Donchev, A. G.; Galkin, N.; Illarionov, A.; Olevanov, M.; Ozirin, V.; Queen, C.; Tarasov, V. *Proc. Natl. Acad. Sci. U.S.A.* **2008**, *105*, 10378–10383.

(11) Raha, K.; Peters, M. B.; Wang, B.; Yu, N.; Wollacott, A. M.; Westerhoff, L. M.; Merz, K. M. *Drug Discovery Today* **2007**, *12*, 725–731.

(12) Raha, K.; Merz, K. M. *J. Am. Chem. Soc.* **2004**, *126*, 1020–1021.

(13) Raha, K.; Merz, K. M. *J. Med. Chem.* **2005**, *48*, 4558–4575.

(14) Fukuzawa, K.; Mochizuki, Y.; Tanaka, S.; Kitaura, K.; Nakano, T. *J. Phys. Chem. B* **2006**, *110*, 16102–16110.

(15) Nakanishi, I.; Fedorov, D. G.; Kitaura, K. *Proteins: Struct., Funct., Bioinf.* **2007**, *68*, 145–158.

(16) Zhang, D. W.; Xiang, Y.; Zhang, J. Z. H. *J. Phys. Chem. B* **2003**, *107*, 12039–12041.

(17) Zhang, D. W.; Xiang, Y.; Gao, A. M.; Zhang, J. Z. H. *J. Chem. Phys.* **2004**, *120*, 1145–1148.

(18) Zhang, D. W.; Zhang, J. Z. H. *Int. J. Quantum Chem.* **2005**, *103*, 246–257.

(19) Mei, Y.; Xiang, Y.; Zhang, D. W.; Zhang, J. Z. H. *Proteins: Struct., Funct., Bioinf.* **2005**, *59*, 489–495.

(20) He, X.; Mei, Y.; Xiang, Y.; Zhang, D. W.; Zhang, J. Z. H. *Proteins: Struct., Funct., Bioinf.* **2005**, *61*, 423–432.

(21) Wu, E. L.; Mei, Y.; Han, K.; Zhang, J. Z. H. *Biophys. J.* **2007**, *92*, 4244–4253.

(22) Bettens, R. P. A.; Lee, A. M. *Chem. Phys. Lett.* **2007**, *449*, 341–346.

(23) Jurecka, T.; Sponer, J.; Cerny, J.; Hobza, P. *Phys. Chem. Chem. Phys.* **2006**, *8*, 1985–1993.

(24) Giese, T. J.; York, D. M. *J. Chem. Phys.* **2004**, *120*, 9903–9906.

(25) Söderhjelm, P.; Aquilante, F.; Ryde, U. *J. Phys. Chem. B* **2009**, *113*, 11085–11094.

(26) Weber, P. C.; Ohlendorf, D. H.; Wendolowski, J. J.; Salemme, F. R. *Science* **1989**, *243*, 85–88.

(27) Weber, P. C.; Wendoloski, J. J.; Pantoliano, M. W.; Salemme, F. R. *J. Am. Chem. Soc.* **1992**, *114*, 3197–3200.

(28) Pugliese, L.; Coda, A.; Malcovati, M.; Bolognesi, M. *J. Mol. Biol.* **1993**, *231*, 698–710.

(29) Livnah, O.; Bayer, E. A.; Wilchek, M.; Sussman, J. L. *Proc. Natl. Acad. Sci. U.S.A.* **1993**, *90*, 5076–5080.

(30) Green, N. M. *Biochem. J.* **1966**, *101*, 774–780.

(31) Green, N. M. *Adv. Protein Chem.* **1975**, *29*, 85–133.

(32) Green, N. M. *Methods Enzymol.* **1990**, *184*, 51–67.

(33) Miyamoto, S.; Kollman, P. A. *Proteins: Struct., Funct., Genet.* **1993**, *16*, 226–245.

(34) Wang, J.; Dixon, R.; Kollman, P. A. *Proteins: Struct., Funct., Genet.* **1999**, *34*, 69–81.

(35) Kuhn, B.; Kollman, P. A. *J. Med. Chem.* **2000**, *43*, 3786–3791.

(36) Kuhn, B.; Gerber, P.; Schulz-Gasch, T.; Stahl, M. *J. Med. Chem.* **2005**, *48*, 4040–4048.

(37) Brown, S. P; Muchmore, S. W. *J. Chem. Inf. Model.* **2006**, *46*, 999–1005.

(38) Weis, A.; Katebzadeh, K.; Söderhjelm, P.; Nilsson, I.; Ryde, U. *J. Med. Chem.* **2006**, *49*, 6596–6606.

(39) Genheden, S.; Ryde, U. *J. Comput. Chem.* **2010**, *31*, 837–846.

(40) Gagliardi, L.; Lindh, R.; Karlström, G. *J. Chem. Phys.* **2004**, *121*, 4494–4500.

(41) Zhang, D. W.; Zhang, J. Z. H. *J. Chem. Phys.* **2003**, *119*, 3599–3605.

(42) Riley, K. E.; Hobza, P. *J. Phys. Chem. A* **2007**, *111*, 8257–8263.

(43) Cornell, W.; Cieplak, P.; Bayly, C.; Gould, I.; Merz, K. M.; Ferguson, D.; Spellmeyer, D.; Fox, T.; Caldwell, J.; Kollman, P. A. *J. Am. Chem. Soc.* **1995**, *117*, 5179–5197.

(44) Duan, Y.; Wu, C.; Chowdhury, S.; Lee, M. C.; Xiong, G.; Zhang, W.; Yang, R.; Cieplak, P.; Luo, R.; Lee, T. *J. Comput. Chem.* **2003**, *24*, 1999–2012.

(45) Cieplak, P.; Caldwell, J.; Kollman, P. A. *J. Comput. Chem.* **2001**, *22*, 1048–1057.

(46) Karlström, G.; Lindh, R.; Malmqvist, P.-Å.; Roos, B. O.; Ryde, U.; Veryazov, V.; Widmark, P.-O.; Cossi, M.; Schimmelpfennig, B.; Neograd, P.; Seijo, L. *Comput. Mater. Sci.* **2003**, *28*, 222–239.

(47) Beebe, N. H. F.; Linderberg, J. *Int. J. Quantum Chem.* **1977**, *12*, 683–705.

(48) Koch, H.; Sánchez de Merás, A.; Pedersen, T. B. *J. Chem. Phys.* **2003**, *118*, 9481–9484.

(49) Aquilante, F.; Pedersen, T. B.; Lindh, R. *J. Chem. Phys.* **2007**, *126*, 194106.

(50) Senn, H. M.; Thiel, W. *Angew. Chem., Int. Ed.* **2009**, *48*, 1198–1229.

(51) Warshel, A.; Levitt, M. *J. Mol. Biol.* **1976**, *103*, 227–249.

(52) Stouch, T. R.; Williams, D. E. *J. Comput. Chem.* **1992**, *13*, 622–632.

(53) Reynolds, C. A.; Essex, J. W.; Richards, W. G. *J. Am. Chem. Soc.* **1992**, *114*, 9075–9079.

(54) Sigfridsson, E.; Ryde, U.; Bush, B. L. *J. Comput. Chem.* **2002**, *23*, 351–364.

(55) Söderhjelm, P.; Ryde, U. *J. Comput. Chem.* **2009**, *30*, 750–760.

(56) Case, D. A.; Darden, T. A.; Cheatham, T. E.; Simmerling, C. L.; Wang, J.; Duke, R. E.; Luo, R.; Crowley, M.; Walker,

R. C.; Zhang, W.; Merz, K. M. ; Wang, B.; Hayik, S.; Roitberg, A.; Seabra, G. ; Kolossváry, I.; Wong, K. F.; Paesani, F.; Vanicek, J.; Wu, X.; Brozell, S. R.; Steinbrecher, T.; Gohlke, H.; Yang, L.; Tan, C.; Mongan, J.; Hornak, V.; Cui, G.; Mathews, D. H.; Seetin, M. G.; Sagui, C.; Babin, V.; Kollman, P. A. *AMBER 10*; University of California: San Francisco, CA, 2008.

(57) Bandyopadhyay, P.; Gordon, M. S.; Mennucci, B.; Tomasi, J. *J. Chem. Phys.* **2002**, *116*, 5023–5032.

(58) Cances, E.; Mennucci, B.; Tomasi, J. *J. Chem. Phys.* **1997**, *107*, 3032–3041.

(59) Frisch, A. E.; Frisch, M. J.; Trucks, G. W. *Gaussian 03 User'S Reference*; Gaussian, Inc.: Wallingford, CT, 2003; p 205.

(60) Li, H.; Pomelli, C. S.; Jensen, J. H. *Theor. Chem. Acc.* **2003**, *109*, 71–84.

(61) Schmidt, M. W.; Baldridge, K. K.; Boatz, J. A.; Elbert, S. T.; Gordon, M. S.; Jensen, J. H.; Koseki, S.; Matsunaga, N.; Nguyen, K. A.; Su, S.; Windus, T. L.; Dupuis, M.; Montgomery, J. A. *J. Comput. Chem.* **1993**, *14*, 1347–1363.

(62) Barone, V.; Cossi, M.; Tomasi, J. *J. Chem. Phys.* **1997**, *107*, 3210–3221.

(63) Frisch, M. J.; Trucks, G. W.; Schlegel, H. B.; Scuseria, G. E.; Robb, M. A.; Cheeseman, J. R.; Montgomery, J. A., Jr.; Vreven, T.; Kudin, K. N.; Burant, J. C.; Millam, J. M.; Iyengar, S. S.; Tomasi, J.; Barone, V.; Mennucci, B.; Cossi, M.; Scalmani, G.; Rega, N.; Petersson, G. A.; Nakatsuji, H.; Hada, M.; Ehara, M.; Toyota, K.; Fukuda, R.; Hasegawa, J.; Ishida, M.; Nakajima, T.; Honda, Y.; Kitao, O.; Nakai, H.; Klene, M.; Li, X.; Knox, J. E.; Hratchian, H. P.; Cross, J. B.; Bakken, V.; Adamo, C.; Jaramillo, J.; Gomperts, R.; Stratmann, R. E.; Yazyev, O.; Austin, A. J.; Cammi, R.; Pomelli, C.; Ochterski, J. W.; Ayala, P. Y.; Morokuma, K.; Voth, G. A.; Salvador, P.; Dannenberg, J. J.; Zakrzewski, V. G.; Dapprich, S.; Daniels, A. D.; Strain, M. C.; Farkas, O.; Malick, D. K.; Rabuck, A. D.; Raghavachari, K.; Foresman, J. B.; Ortiz, J. V.; Cui, Q.; Baboul, A. G.; Clifford, S.; Cioslowski, J.; Stefanov, B. B.; Liu, G.; Liashenko, A.; Piskorz, P.; Komaromi, I.; Martin, R. L.; Fox, D. J.; Keith, T.; Al-Laham, M. A.; Peng, C. Y.; Nanayakkara, A.; Challacombe, M.; Gill, P. M. W.; Johnson, B.; Chen, W.; Wong, M. W.; Gonzalez, C. Pople, J. A. *Gaussian 03*, Revision D.01; Gaussian, Inc.: Wallingford CT, 2004.

(64) Marenich, A. V.; Olson, R. M.; Kelly, C. P.; Cramer, C. J.; Truhlar, D. G. *J. Chem. Theory Comput.* **2007**, *3*, 2011–2033.

(65) Kelly, C. P.; Cramer, C. J.; Truhlar, D. G. *J. Phys. Chem. B* **2006**, *110*, 16066–16081.

(66) Wolfenden, R.; Andersson, L.; Cullis, P. M.; Southgate, C. C. B. *Biochemistry* **1981**, *20*, 849–855.

(67) Sitkoff, D.; Sharp, K. A.; Honig, B. *J. Phys. Chem.* **1994**, *98*, 1978–1988.

(68) Florián, J; Warshel, A. *J. Phys. Chem. B* **1997**, *101*, 5583–5595.

(69) Kongsted, J.; Söderhjelm, P.; Ryde, U. *J. Comput.-Aided Mol. Des.* **2009**, *23*, 395–409.

(70) Fratev, F.; Jonsdottir, S. O; Mihaylova, E.; Pajeva, I. *Mol. Pharmaceutics* **2009**, *6*, 144–157.

(71) Grazioso, G.; Cavalli, A.; de Amici, M.; Recanatini, M.; de Micheli, C. *J. Comput. Chem.* **2008**, *29*, 2593–2603.

(72) Fogolari, F.; Moroni, E.; Wojciechowski, M.; Baginski, M.; Ragona, L.; Molinari, H. *Proteins* **2005**, *59*, 91–103.

(73) Gilson, M. K; Honig, B. *Proteins: Struct., Funct., Genet.* **1998**, *4*, 7–18.

(74) Hermann, R. B. *J. Phys. Chem.* **1972**, *76*, 2754–2759.

(75) Swanson, J. M. J.; Henchman, R. H.; McCammon, J. A. *Biophys. J.* **2004**, *86*, 67–74.

(76) Gräter, F.; Schwarzl, S. M.; Dejaegere, A.; Fischer, S.; Smith, J. C. *J. Phys. Chem. B* **2005**, *109*, 10474–10483.

(77) Wang, M. L.; Wong, C. F. *J. Chem. Phys.* **2007**, *126*, 026101.

(78) Kaukonen, M.; Söderhjelm, P.; Heimdal, J.; Ryde, U. *J. Phys. Chem. B* **2008**, *112*, 12537–12548.

(79) Kongsted, J.; Ryde, U. *J. Comput.-Aided Mol. Des.* **2009**, *23*, 63–71.

(80) Morris, G. M.; Goodsell, D. S.; Halliday, R. S.; Huey, R.; Hart, W. E.; Belew, R. K.; Olson, A. J. *J. Comput. Chem.* **1998**, *19*, 1639–1662.

(81) Huey, R.; Morris, G. M.; Olson, A. J.; Goodsell, D. S. *J. Comput. Chem.* **2007**, *28*, 1145–1152.

(82) Cossi, M.; Tomasi, J.; Cammi, R. *Int. J. Quant. Chem. Quant. Chem. Symp.* **1995**, *29*, 695–702.

(83) Pullman, B. *Intermolecular Interactions, from diatomics to biomolecules*; John Wiley & Sons: Chichester, U.K., 1978; p 69.

(84) Pierotti, R. A. *Chem. Rev.* **1976**, *76*, 717–726.

(85) Caillet, J.; Claverie, P. *Acta Crystallogr., Sect. B* **1978**, *34*, 3266–3273.

(86) Floris, F.; Tomasi, J. *J. Comput. Chem.* **1989**, *10*, 616–627.

(87) Tan, C.; Tan, Y.-H.; Luo, R. *J. Phys. Chem. B* **2007**, *111*, 12263–12274.

(88) Chandler, D.; Andersen, H. C. *J. Chem. Phys.* **1972**, *57*, 1930–1937.

(89) Kovalenko, A.; Hirata, F. *J. Chem. Phys.* **2000**, *112*, 10391–10417.

(90) Genheden, S.; Luchko, T.; Gusarov, S.; Kovalenko, A.; Söderhjelm, P.; Ryde, U. An MM/3D-RISM approach for ligand-binding affinities. *J. Phys. Chem. B*, Submitted.

(91) Cossi, M; Barone, V; Cammi, R; Tomasi, J. *Chem. Phys. Lett.* **1996**, *255*, 327–335.

(92) DeChancie, J.; Houk, K. N. *J. Am. Chem. Soc.* **1999**, *129*, 5419–5429.

CT9006986